Epitaxial InN/InGaN quantum dots on Si: Cl^- anion selectivity and pseudocapacitor behavior

Paul E. D. Soto Rodriguez , Claudio Maria Mari , Stefano Sanguinetti , Riccardo Ruffo , and Richard Nötzel

Epitaxial InN quantum dots (QDs) on In-rich InGaN, applied as an electrochemical electrode, activate Cl^--anion-selective surface attachment, bringing forth faradaic/pseudocapacitor-like behavior. In contrast to traditional pseudocapacitance, here, no chemical reaction of the electrode material occurs. The anion attachment is explained by the unique combination of the surface and quantum properties of the InN QDs. A high areal capacitance is obtained for this planar electrode together with rapid and reversible charge/discharge cycles. With the growth on cheap Si substrates, the InN/InGaN QD electrochemical electrode has great potential, opening up new application fields for III–nitride semiconductors.

Ion-selective electrodes are commonly used as sensors for measuring ionic concentrations in analytical chemistry and biochemical research. Owing to their capability to take up of ions, their application as an electrochemical energy storage device is proposed. The field of electrochemical energy storage devices is dominated by batteries with high energy density. Supercapacitors, on the other hand, are high-capacitance electrochemical capacitors with high power density, thus bridging the gap between conventional capacitors and rechargeable batteries when fast storage and delivery of large amounts of energy are required. Supercapacitors are classified into electrostatic double-layer capacitors (EDLCs), pseudocapacitors, and hybrid capacitors. The charge storage in EDLCs is in the Helmholtz double layer at the electrode–electrolyte interface, which is achieved without involving chemical reactions. The charge storage in pseudocapacitors, which can be much more efficient, is achieved by faradaic charge-transfer processes (redox reactions, intercalation, and electrosorption) in, for example, batteries, which are, however, faster and more reversible in near-surface regions of the electrode.

We found the unique anion-selective nature of epitaxial InN quantum dots (QDs) (islands) grown on compact, In-rich InGaN layers on Si(111) substrates by plasma-assisted molecular beam epitaxy (PAMBE) forming planar electrodes with pronounced faradaic/pseudocapacitor-like behavior. However, no chemical reaction of the electrode material occurs, which is fundamentally different from traditional pseudocapacitor electrode materials such as metal oxides.[1–7] Instead, the pseudocapacitance originates from pure anion surface attachment with the QDs as sole active sites owing to a unique combination of surface charge and quantum properties, as shown in Fig. 1(a) (the model will be described in detail after the experimental sections). The quasi-planar InN/InGaN QD electrode exhibits a high areal capacitance of $\sim 9000\,\mu F \cdot cm^{-2}$ in 1 M KCl aqueous solution, while much lower ones in KBr and KF aqueous electrolytes, and rapid and reversible charge/discharge cycles. No faradaic/pseudocapacitor-like behavior is observed with the usual organic electrolytes used to increase the voltage limit and, thus, the energy density. All InN/InGaN QD electrodes are directly grown on cheap Si substrates,[8,9] boosting their application potential for electrochemical devices as a whole.

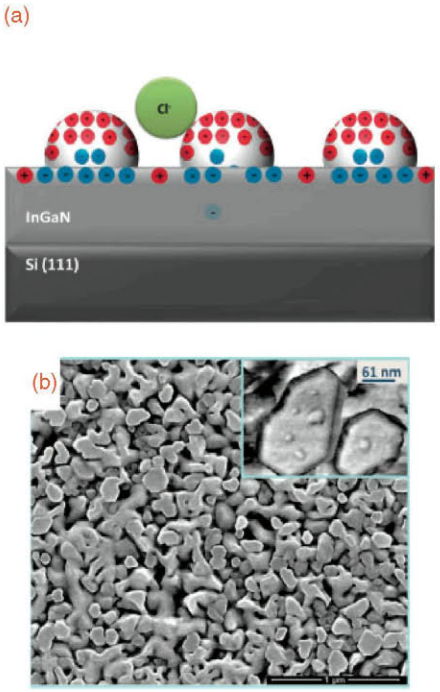

Fig. 1. (a) Scheme of the InN/InGaN QD structure and Cl^- ion attachment. (b) SEM image of the InGaN layer. Inset: AFM image of the InN QDs on the InGaN layer.

InGaN growth was by PAMBE (MECA 2000). The p-type Si(111) wafers were first nitrided at 850 °C for 5 min by exposure to an active N_2 flux of 7.16×10^{14} atoms s^{-1} cm^{-2}. The active N_2 flux was kept the same during both nitration and growth performed for 1 h at 450 °C. The In and Ga fluxes were 3.33 and 1.23×10^{14} atoms s^{-1} cm^{-2}, respectively.

The morphologies of the InGaN layer and InN QDs were studied by scanning electron microscopy (SEM) and atomic force microscopy (AFM), respectively. The In content was determined by high-resolution X-ray diffraction (HRXRD) reciprocal space mapping, while the surface chemical properties by Fourier transform infrared (FTIR) spectroscopy in an attenuated total reflectance (ATR) configuration. Electrochemical assessment was performed by cyclic voltammetry (CV) and galvanostatic cycling with potential limitation (GCPL). Owing to the high n-type electrical conductivity of

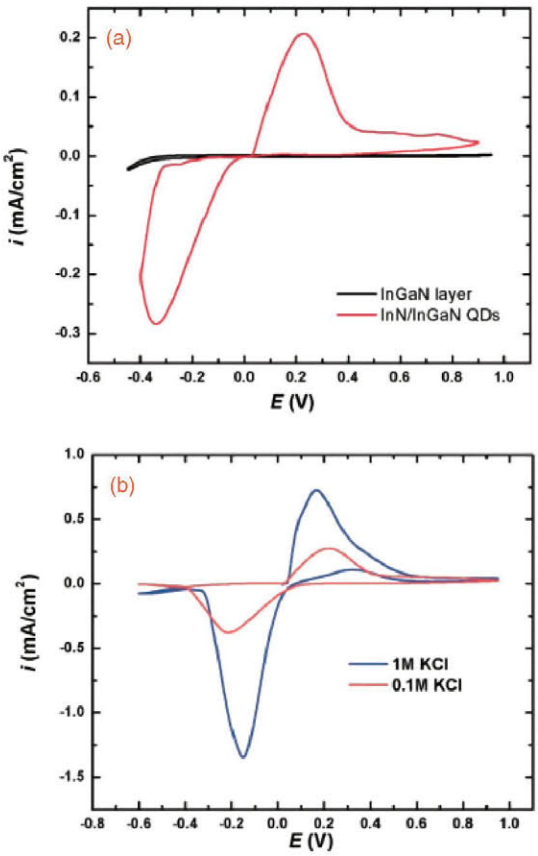

Fig. 2. (a) CV curves of the InGaN (black) and InN/InGaN QD (red) electrodes in 0.1 M KCl aqueous electrolyte. The scan rate is 20 mV s^{-1}. (b) CV curves of the InN/InGaN QD electrode in 0.1 M (orange) and 1 M (blue) KCl aqueous electrolytes. The scan rate is 20 mV s^{-1}.

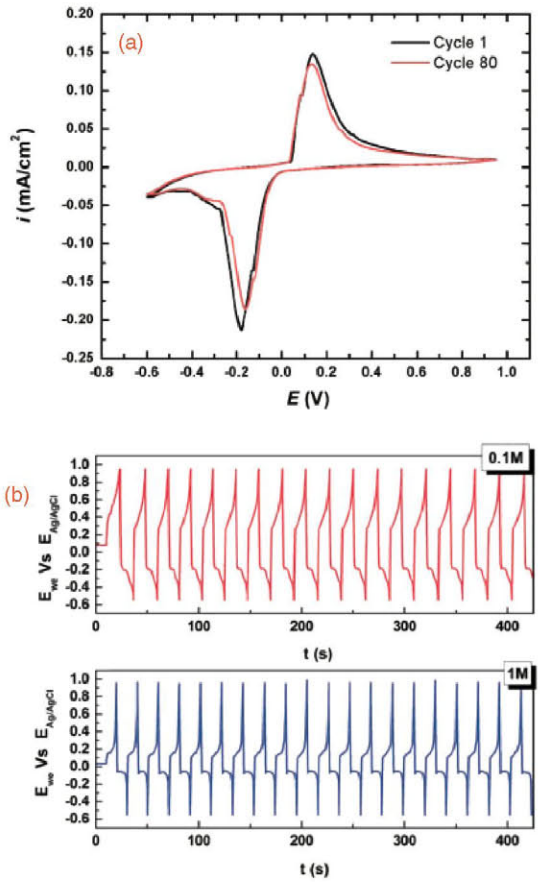

Fig. 3. (a) CV curves (scan rate 200 mV s^{-1}) of the InN/InGaN QD electrode after 1 (black) and 80 (red) cycles in 0.1 M KCl aqueous electrolyte. (b) GCPL measurements of the InN/InGaN QD electrode in 0.1 M (red) and 1 M (blue) KCl aqueous electrolytes. The fixed current is 50 μA.

In-rich InGaN, silver paste contacts were used. The measurements were performed in a three-electrode configuration with the InN/InGaN QDs or InGaN layer working electrode, Pt counter electrode, and Ag/AgCl reference electrode, using a VMP3 potentiostat from Biologic. The working electrode's surface area exposed to the electrolyte was 0.0706 cm^2. KCl was ACS reagent grade from Sigma-Aldrich. KBr and KF were proanalysis grade from Merck.

In Fig. 1(b), a SEM image of the InGaN layer without QDs and an AFM image in the inset, with enlarged scale, displaying the InN QDs are presented. The InGaN layer is compact with a *c*-plane island structure on which the InN QDs are clearly visible. Statistical analysis of many AFM images gives a QD density of 7×10^9 QDs cm^{-2}, diameters ranging from 10 to 40 nm, and heights of 2–4 nm.[9] The In content of the InGaN layer, obtained from HRXRD reciprocal space mapping, is 73%. The InGaN layer is fully relaxed.

Figures 2(a) and 2(b) show the CV curves obtained at a 20 mV s^{-1} scan rate in 0.1 M KCl aqueous electrolyte. As required for reversible pseudocapacitance, the applied voltage range is below the onset of electrolysis of the electrolyte or water. Hence, there are no electrochemical reactions at the electrodes; consequently, no gas bubbles evolve. The InGaN layer CV curve shows only a capacitive current due to electrostatic double-layer capacitance. In contrast, for the InN/InGaN QDs, the marked faradaic current peaks indicate the pseudocapacitor-like behavior. FTIR spectroscopy reveals no chemical modification of the InN/InGaN QD surface as expected for the well-known chemical stability of InGaN (results not shown). Hence, the active sites for the faradaic/pseudocapacitor behavior are solely the QDs established by their anion-selective nature, i.e., the attraction and attachment of anions to the QD surface. The origin of faradaic currents will be explained in our model below, originating solely from the electron exchange between the QDs and the bulk electrode as there are no chemical reactions of neither the electrolye or water nor the electrode itself. In order to demonstrate the effect of electrolyte concentration, the CV curves for 0.1 and 1 M KCl solutions are shown in Fig. 2(b). A clear increase in current density is observed in the 1 M KCl solution owing to the lower internal resistance.

To confirm the stability of the InN/InGaN QD electrode, the CV curves after the 1st and 80th cycle in 0.1 M KCl electrolyte are compared in Fig. 3(a). The observed evolution of the curves is small. No qualitative differences are observed. This is the same as that of the FTIR spectra. Only the as-prepared electrode is cleaner. In addition, an excellent reversibility is revealed in Fig. 3(b) in the symmetric charge/discharge cycles assessed using the GCPL technique in 0.1 and 1 M KCl aqueous solutions. The nonlinear slope clearly identifies the faradaic/pseudocapacitor-like behavior. The charge/discharge cycling is faster for the higher KCl concentration again owing to the lower internal resistance.

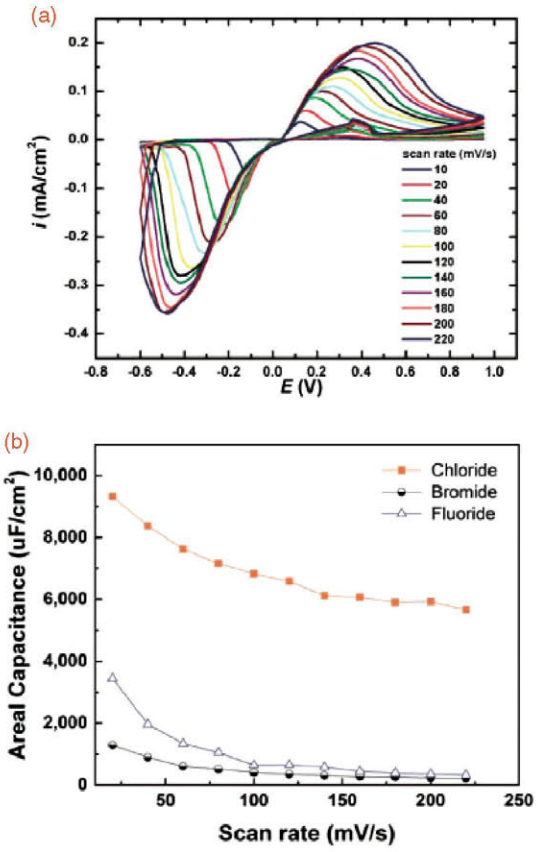

Fig. 4. (a) CV curves of the InN/InGaN QD electrode in 1 M KCl aqueous electrolyte at different scan rates. (b) Areal capacitance as a function of scan rate in 1 M KCl, KBr, and KF aqueous electrolytes.

The capacitance C is determined from the CV curves at different scan rates for the 1 M KCl aqueous solution, shown in Fig. 4(a), according to the following equation.

$$C = \frac{\int I(E)\,dE}{2v\Delta E}$$

$I(E)$ is the current at the electrode potential E, v is the scan rate, and ΔE is the electrode potential window in which the scan is performed.

As commonly observed, the capacitance depends on the scan rate due to limited ion transport in the electrolyte.[10,11] The areal capacitance decreases from 9320 μF cm^{-2} for the scan rate of 20 mV s^{-1} to 5669 μF cm^{-2} for the scan rate of 220 mV s^{-1}, as shown in Fig. 4(b). The areal capacitance is twice that of carbon-based materials[10] and one order of magnitude larger than that of metal oxides.[7] Of course, the projected areal capacitance of three-dimensional (3D) network structures[11] can be very large, but cannot be compared directly with that of 2D electrodes. Capacitance per volume would be more indicative in that case.

The capacitances for other aqueous electrolytes, i.e., KBr and KF, also shown in Fig. 4(b), are much lower, and some commonly tested organic electrolytes, such as 1 M $LiClO_4$, $LiBF_4$, and $LiPF_6$, dissolved in acetonitrile show no pseudocapacitor behavior. This points to an optimum anion size for the attachment to the QDs. For very large anions, the attachment might become too weak, and for very small anions, the attachment might be too strong, and thus also electrostatically between the QDs (smaller EDLC). The performance in the Cl^--ion-based aqueous electrolyte is by far the best. This is a very important result of technological relevance as the Cl^--based aqueous electrolyte is cheap, the least toxic, and easy to handle. Moreover, the high affinity of the InN/InGaN QDs toward CL^- ions is very interesting because it opens new promising solutions for wastewater treatment and for the chlor-alkali industry.

For supercapacitors, the common benchmark is specific capacitance, i.e., the capacitance per weight of an active material. Calculating the weight of the InN QDs, being the sole active centers, from their volume and density, determined from AFM (and alternatively from the known amount of the deposited material), we obtain specific capacitances between 182 000 and 111 000 F g^{-1} for the scan rates between 20 and 220 mV s^{-1}. Owing to the low QD mass, these values are two to three orders of magnitude larger than the best ones reported in the literature for traditional pseudocapacitor electrode materials. The reason for these unrealistically high values is that, for traditional materials, the pseudocapacitance originates from electrochemical reactions penetrating into the bulk, while for our InN/InGaN QDs, the pseudocapacitor-like behavior originates solely from the attachment of anions on the QD surface without the chemical reaction of InN. This means that the concepts of specific capacitance/mass loading are not applicable to the InN/InGaN QDs where only the high nanostructure surface-to-volume ratio counts, highlighting the fundamentally different origin of pseudocapacitance.

The strong anion attachment is explained by the high (the highest known) density of intrinsic positively charged surface donor states [(2–3) × 10^{13} cm^{-2}] of c-plane InN[12,13] together with the zero-dimensional electronic properties of the QDs. To be more quantitative, we take the QD imaged in Fig. 2 of Ref. 9 with a base width of 10 nm and a height of 3 nm. For a circular shape and a surface donor density of 2 × 10^{13} cm^{-2}, 16 donors are situated on the QD surface (approximated by a circular disk). A QD of this size has a limited number of bound states, likely four,[14] which can accommodate eight electrons (the energetics of our InN/InGaN QDs[9] is very similar to that of InAs/GaAs QDs[14]). Hence, eight surface donors are uncompensated with the remaining eight electrons quantum mechanically repelled to the InGaN barrier layer underneath the QD forming an electric dipole with the exposed positive net surface charge. This quantum repulsion overcomes the Debye screening length in the electron surface accumulation layer (attracted by the donors), which is much smaller (~1 nm) than the QD width for such high carrier concentrations. Moreover, approximating the surface and base of the QD by two oppositely charged (eight elementary charges each) circular disks of 5 nm radius, separated by 3 nm, leads to a potential difference of 150 mV. This quantitatively accounts for the anion-selective behavior due to the Coulomb attraction of anions, which is reversible, upon external voltage application, and generates the observed faradaic/pseudocapacitor-like behavior: For each attached/detached anion, one electron is released/captured by the QD. There is neither direct electron charge transfer from the electrolyte to the electrode material (no electrochemical reactions of the electrolyte or water) nor chemical reactions of the electrode. The electron charge transfer is between the QD — the "artificial atom" — and the bulk of the electrode, which can be viewed as an 'artificial redox reaction', as

shown in Fig. 1(a). This nicely complements the superior performance of InN/InGaN QDs as a biosensor transducer and photoelectrode for water splitting[15,16] which originates from electrocatalytic oxidation enhancement,[13] i.e., Coulomb attraction and transfer of electrons.

To conclude, epitaxial InN QDs on In-rich InGaN have been demonstrated as a key for the anion-selective nature, bringing forth a faradaic/pseudocapacitor-like behavior. The best performance is obtained in KCl aqueous solutions. The high areal capacitance of this planar electrode of $\sim 9000\,\mu F\,cm^{-2}$ is superior to that of metal oxides. Rapid and reversible charge/discharge cycles are observed, and there is no chemical reaction of the electrode material in contrast to traditional pseudocapacitor electrode materials. The pseudocapacitance is due to Coulomb attraction and the attachment of Cl^- ions solely to the QDs.

Acknowledgments Paul E. D. Soto Rodriguez thanks V. J. Gómez and P. Aseev for technical support for HRXRD and AFM measurements.

1) B. E. Conway, *Electrochemical Supercapacitors, Scientific Fundamentals and Technological Applications* (Plenum, New York, 1999).
2) S. Chen, R. Ramachandran, V. Man, and R. Saraswathi, Int. J. Electrochem. Sci. **9**, 4072 (2014).
3) V. V. N. Obreja, AIP Conf. Proc. **98**, 1597 (2014).
4) Z. Wu, G. Zhou, L. Yin, W. Ren, F. Li, and H. Cheng, Nano Energy **1**, 107 (2012).
5) M. Mastragostino, C. Arbizzani, and F. Soavi, J. Power Sources **97–98**, 812 (2001).
6) S. Yoon, E. Kang, J. K. Kim, C. W. Lee, and J. Lee, Chem. Commun. **47**, 1021 (2011).
7) A. Burke, J. Power Sources **91**, 37 (2000).
8) P. Aseev, P. E. D. Soto Rodriguez, V. J. Gómez, N. H. Alvi, J. M. Mánuel, F. M. Morales, J. J. Jiménez, R. García, A. Senichev, C. Lienau, E. Calleja, and R. Nötzel, Appl. Phys. Lett. **106**, 072102 (2015).
9) P. E. D. Soto Rodriguez, P. Aseev, V. J. Gómez, P. Kumar, N. H. Alvi, E. Calleja, J. M. Mánuel, F. M. Morales, J. J. Jiménez, R. García, A. Senichev, C. Lienau, and R. Nötzel, Appl. Phys. Lett. **106**, 023105 (2015).
10) A. Arslan and E. Hür, Int. J. Electrochem. Sci. **7**, 12558 (2012).
11) L. Hu, W. Chen, X. Xie, N. Liu, Y. Yang, H. Wu, Y. Yao, M. Pasta, H. N. Alshareef, and Y. Cui, ACS Nano **5**, 8904 (2011).
12) C. G. Van de Walle and D. Segev, J. Appl. Phys. **101**, 081704 (2007).
13) P. E. D. Soto Rodriguez, V. Calderon Nash, P. Aseev, V. J. Gómez, P. Kumar, N. H. Alvi, A. Sánchez, R. Villalonga, J. M. Pingarrón, and R. Nötzel, Electrochem. Commun. **60**, 158 (2015).
14) L. W. Wang, J. Kim, and A. Zunger, Phys. Rev. B **59**, 5678 (1999).
15) N. H. Alvi, P. E. D. Soto Rodriguez, V. J. Gómez, P. Kumar, G. Amin, O. Nur, M. Willander, and R. Nötzel, Appl. Phys. Lett. **101**, 153110 (2012).
16) N. H. Alvi, P. E. D. Soto Rodriguez, P. Aseev, V. J. Gómez, A. H. Alvi, W. U. Hassan, M. Willander, and R. Nötzel, Nano Energy **13**, 291 (2015).